

# Tre1 GPCR initiates germ cell transepithelial migration by regulating *Drosophila melanogaster* E-cadherin

Prabhat S. Kunwar,<sup>1,2</sup> Hiroko Sano,<sup>1,2</sup> Andrew D. Renault,<sup>1,2</sup> Vitor Barbosa,<sup>1,2</sup> Naoyuki Fuse,<sup>3</sup> and Ruth Lehmann<sup>1,2</sup>

<sup>1</sup>Howard Hughes Medical Institute and <sup>2</sup>Kimmel Center for Biology and Medicine at the Skirball Institute for Biomolecular Medicine, Department of Cell Biology, New York University School of Medicine, New York, NY 10016

<sup>3</sup>Global Center of Excellence Program, Division of Biological Science, Kyoto University, Kyoto 606-8502, Japan

**D**espite significant progress in identifying the guidance pathways that control cell migration, how a cell starts to move within an intact organism, acquires motility, and loses contact with its neighbors is poorly understood. We show that activation of the G protein-coupled receptor (GPCR) trapped in endoderm 1 (Tre1) directs the redistribution of the G protein G $\beta$  as well as adherens junction proteins and Rho guanosine triphosphatase from the cell periphery to the lagging tail of germ cells at the onset of *Drosophila melanogaster* germ cell migration. Subsequently, Tre1 activity triggers germ cell

dispersal and orients them toward the midgut for directed transepithelial migration. A transition toward invasive migration is also a prerequisite for metastasis formation, which often correlates with down-regulation of adhesion proteins. We show that uniform down-regulation of E-cadherin causes germ cell dispersal but is not sufficient for transepithelial migration in the absence of Tre1. Our findings therefore suggest a new mechanism for GPCR function that links cell polarity, modulation of cell adhesion, and invasion.

## Introduction

Cell migration plays a very important role during a variety of processes such as development, immune defense, and metastasis (Franz et al., 2002; Horwitz and Webb, 2003; Ridley et al., 2003). The coordinated migration of different kinds of cells in space and time gives rise to the three germ layers and the three-dimensional architecture of different organs and organisms. Cells of the immune system migrate through blood vessels and tissues to reach infected sites; and cancer cells migrate away from their tissues of origin to ectopic places during metastasis (Friedl and Wolf, 2003; Sahai, 2005). Thus far, the basic mech-

anisms of cell migration have been elucidated mostly from in vitro studies in solitary cells (Chung et al., 2001; Iijima et al., 2002; Ridley et al., 2003; Van Haastert and Devreotes, 2004). Cell migration in living, multicellular organisms, however, is likely much more complex (Rorth, 2002; Kunwar et al., 2006; Montell, 2006; Raz and Reichman-Fried, 2006). At the onset of directed migration, cells not only have to acquire motility but also have to be able to perceive specific, directional migration cues. During their journey, migrating cells may be required to detect and interpret multiple, possibly conflicting guidance cues, and must coordinate their adhesion to surrounding cells to reorient, pause, and move in a directed fashion while targets change. Finally, at the end, cells have to know when they have reached their target and cease their motility.

Significant progress has been made in identifying guidance molecules, receptors, and intracellular mediators that act during directed migration. G protein-coupled receptors (GPCRs) have been widely studied for their role in directional migration

P.S. Kunwar and H. Sano contributed equally to this paper.

Correspondence to Ruth Lehmann: lehmann@saturn.med.nyu.edu

P.S. Kunwar's present address is Anderson Laboratory, Division of Biology, California Institute of Technology, Pasadena, CA 91125.

H. Sano's present address is Ochanomizu Academic Production, Division of Advanced Sciences, Ochanomizu University, Bunkyo-ku, Tokyo 112-8610, Japan.

A.D. Renault's present address is Max Planck Institute for Developmental Biology, Tübingen, D-72076 Germany.

Abbreviations used in this paper: AEL, after egg laying; DE-cadherin, *Drosophila melanogaster* E-cadherin; EMT, epithelial–mesenchymal transition; GPCR, G protein-coupled receptor; shg, shotgun; tre1, trapped in endoderm 1; tud, tudor; UAS, upstream activation sequence.

The online version of this article contains supplemental material.

© 2008 Kunwar et al. This article is distributed under the terms of an Attribution-Noncommercial-Share Alike-No Mirror Sites license for the first six months after the publication date (see <http://www.jcb.org/misc/terms.shtml>). After six months it is available under a Creative Commons License (Attribution-Noncommercial-Share Alike 3.0 Unported license, as described at <http://creativecommons.org/licenses/by-nc-sa/3.0/>).

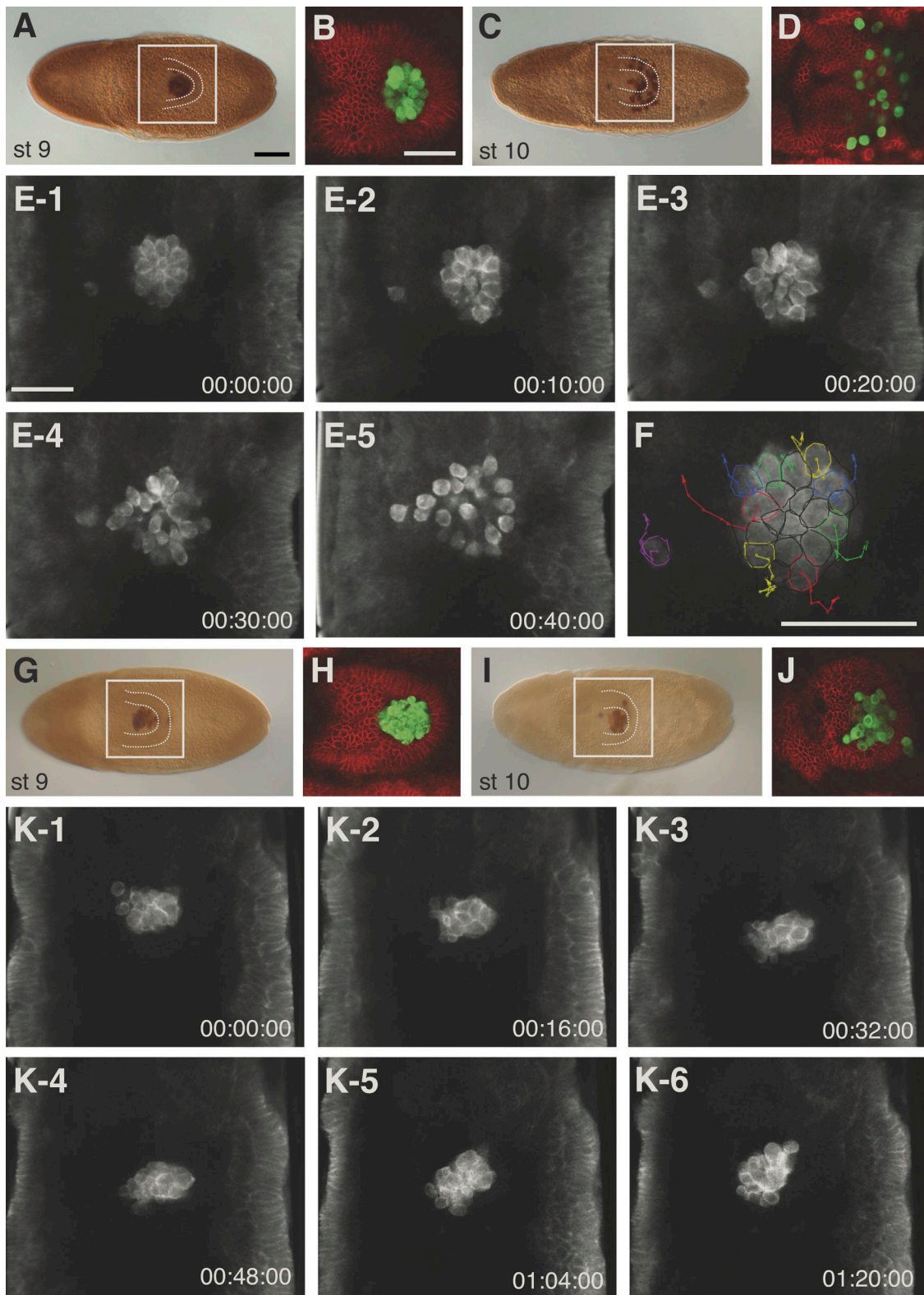


**Figure 1. Live imaging of germ cell migration through the midgut in wild-type and *tre1* mutant embryos.** (A–F) Migration of germ cells in the wild type. (A and C) Wild-type embryos at stages 9 and 10. Germ cells (anti-Vasa antibody, brown) form a tight cluster inside the midgut (dotted lines) at stage 9 (A), then disperse and migrate through the midgut to reach the basal side of the midgut cell layer at stage 10 (C). (B and D) High-magnification confocal images of the regions in the boxes in A and C, respectively, showing the midgut regions of stage 9 (B) and stage 10 embryos (D). Germ cells are shown in green, and the midgut cell membrane was detected with anti-neurotactin antibody (red). (E) Time-lapse analysis of germ cell migration during stages 9 and 10 with two-photon microscopy. Shown are still images from a time-lapse video (Video 3, available at <http://www.jcb.org/cgi/content/full/jcb.200807049/DC1>). Germ cells lose adhesion with other germ cells just before the onset of migration through the midgut (E 3 and 4). (F) Trajectory of germ cells shows radial dispersion. (G–K) Migration of germ cells in *tre1* mutants. (G and I) *tre1* mutant embryos at stages 9 and 10. *tre1* germ cells (brown) form a tight cluster in the midgut at stage 9 (G) similar to the wild

(Doitsidou et al., 2002; Ara et al., 2003; Knaut et al., 2003; Kunwar and Lehmann, 2003; Molyneaux et al., 2003; Kunwar et al., 2006). Cells use GPCRs to detect and migrate toward higher concentrations of chemoattractants. Immune cells and germ cells, for example, express the chemokine receptor CXCR4 and follow the distribution of the chemokine SDF1 (stromal cell-derived factor 1; Doitsidou et al., 2002; Ara et al., 2003; Knaut et al., 2003; Kunwar and Lehmann, 2003; Molyneaux et al., 2003; Kunwar et al., 2006; Boldajipour et al., 2008).

Lymphocytes use sphingosine-1-phosphate receptors to egress from lymphoid tissues, where S1P levels are higher (Zou et al., 1998; Moser et al., 2004; Schwab et al., 2005; Wei et al., 2005). Despite significant progress in identifying the guidance molecules, receptors, and intracellular mediators that act during directed migration, the cellular and molecular mechanisms that initiate cell migration are only poorly understood. At the start of migration, cells need to acquire motility, may lose cell adhesion with neighboring cells, and are required to gain the ability to respond directionally to external cues. The detailed cellular transformations, the temporal sequence of these events, and the relative influence caused by intrinsic and extrinsic cell information are the focus of our study.

*Drosophila melanogaster* germ cells provide a genetically tractable system to visualize and follow individual germ cells as they start directed migration (Santos and Lehmann, 2004; Sano et al., 2005; Kunwar et al., 2006). The onset of directed germ cell migration coincides with the transepithelial migration of germ cells through the primordium of the future midgut. Evidence for a germ cell autonomous function for transepithelial migration came from the identification of a novel GPCR *trapped in endoderm 1* (*tre1*; Kunwar et al., 2003). Maternal *tre1* RNA is present in germ cells, and *tre1* function is required there. General cell motility and the movements of germ cells toward the gonad do not depend on Tre1, which suggests that Tre1 specifically regulates the onset of migration.

To understand the cellular mechanisms underlying the onset of directed migration, we used two-photon imaging to visualize the cellular transformations that occur *in vivo* as germ cells migrate through the midgut epithelium. Comparison of wild-type and *tre1* mutant germ cells suggests that regulated activation of the Tre1 GPCR controls three phases of early migration: polarization of germ cells, dispersal into individual cells, and transepithelial migration. Germ cell polarization leads to a redistribution of cell–cell adherens proteins, such that *D. melanogaster* E-cadherin (DE-cadherin) levels are reduced from the leading edge of the migrating cells and accumulate in the tail region. Tre1 likely signals via the G proteins  $G\gamma 1$  and  $G\beta 13f$  as well as Rho-1, as we detect  $G\beta$  and Rho-1 protein localization in the tail region, and deletion of their function specifically in germ cells causes the same phenotype as mutation in

*tre1*. Our results suggest a novel function for GPCR signaling in initiating cell migration by polarizing the migrating cell. This polarization leads to the redistribution of signaling components and adherens proteins and may trigger cell dispersal and directed migration.

## Results

### Live imaging of early steps in germ cell migration

To visualize germ cell migration in developing embryos, we used two-photon microscopy and a germ cell–specific expression system, which translates the actin-binding domain of Moesin fused to EGFP under the control of *nanos* regulatory sequences (Sano et al., 2005). Germ cells appeared motile soon after their formation at the blastoderm stage (stage 5, 2 h and 10 min to 2 h and 50 min after egg laying [AEL]), as they produced small protrusions away from their neighbors (Video 1, available at <http://www.jcb.org/cgi/content/full/jcb.200807049/DC1>). Despite this apparent motility, germ cells only rarely (1–2 germ cells per embryo) separated from their neighbors and migrated directly through the underlying blastoderm cells (Video 1). Subsequently, during gastrulation (stage 7–8, 3 h to 3 h and 40 min AEL), as germ cells were internalized together with the invaginating posterior midgut primordium, they rounded up and showed less protrusive activity (Video 2). At stage 9 (3 h and 40 min to 4 h and 20 min AEL), germ cells were found inside the midgut primordium in a tight cluster (Fig. 1, A and B); they were in close contact with each other and showed little contact with the surrounding somatic midgut cells (Fig. 1, A and E, 1 and 2; and Video 3). During this stage, germ cells started to reorganize, changed their shape, and took on a highly polarized morphology. Using electron microscopy, a radial organization of germ cells within the midgut was clearly visible, with the large germ cell nuclei pointed toward the midgut while fine membranous material, apparently corresponding to the tail region, filled the inside of the cluster (see Fig. 3 A). This organization oriented the leading edge of each germ cell toward the surrounding midgut primordium. Next, the germ cells lost adhesion to each other, and extensions reached from the germ cells toward the midgut epithelium (Fig. 1 E, 3 and 4; and Fig. S1 A).

Subsequently, germ cells dispersed as they migrated through the midgut primordium to reach the basal side of the midgut cells by stage 10 (4 h and 20 min to 5 h and 20 min AEL; Fig. 1, C, D, and E 5). Long cytoplasmic extensions connected germ cells with each other immediately after the onset of transepithelial migration (Fig. S2 and Video 3, available at <http://www.jcb.org/cgi/content/full/jcb.200807049/DC1>). As germ cells transmigrated through the midgut epithelium, they appeared completely individualized, displayed amoeboid behavior, and were

type. However, *tre1* mutant germ cells are unable to disperse and remain in the midgut (I). High-magnification confocal images of regions in the boxes in G and I, respectively, showing the midgut regions of stage 9 (H) and stage 10 *tre1* mutant embryos (J). Germ cells are shown in green and the membranes of the midgut cells are labeled in red. (K) Still images of *tre1* mutant embryo during stages 9 and 10 from time-lapse analysis shown in Video 5. Germ cells are motile and change their positions; however, they are not able to disperse and remain in a tight group in the midgut. Embryos are oriented anterior to the left, dorsal view in A–D and G–J. Embryos in E and K are oriented anterior to the top, dorsal view. Bars, 50  $\mu$ m.

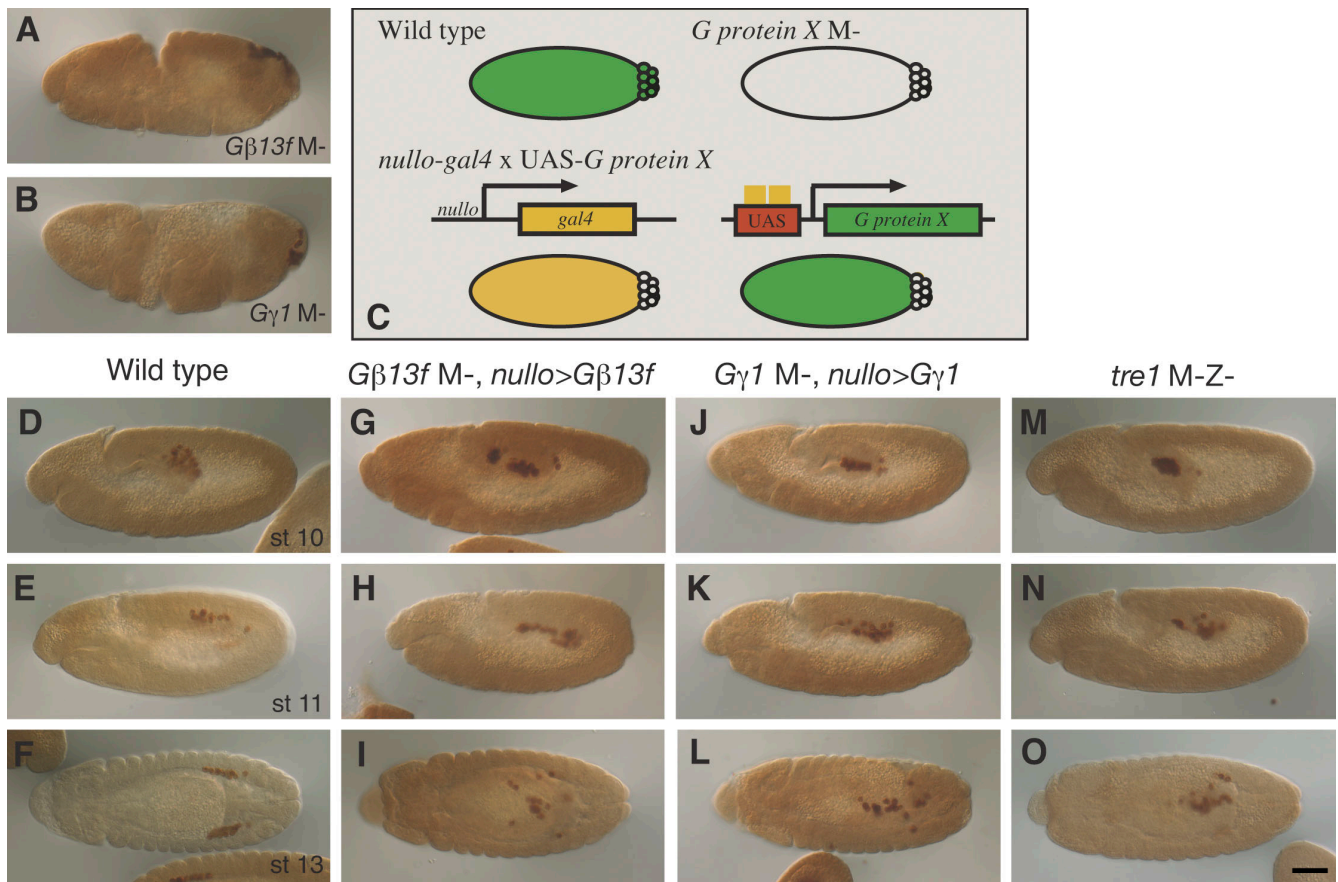


**Figure 2. *Gβ13f* and *Gy1* act downstream of *tre1* in transepithelial migration.** (A and B) Phenotype of maternal *Gβ13f* and *Gy1* mutants. Loss of maternal *Gβ13f* and *Gy1* results in gastrulation defects and prevents normal germ cell migration. (C) A strategy to rescue the gastrulation phenotype by overexpression of G proteins in the somatic tissue. In the wild type, the product of the *G protein X* (green) is provided maternally in germ cells and the soma, and is lost from both tissues in maternal *G protein X* mutants. *G protein X* product is restored only in the soma by using a soma-specific Gal4 transgene, *nullo-GAL4* (yellow), which binds to UAS to turn on transcription in the soma but not in germ cells. (D–O) Phenotype of germ cell migration in the wild type (D–F) and maternal *Gβ13f* (G–I) and *Gy1* (J–L) mutants with somatic rescue. In these mutants, germ cells (brown, anti-Vasa antibody) display a transepithelial migration defect similar to *tre1* mutants (M–O). Embryos are oriented anterior to the left, lateral views except for stage 13 embryos, which are oriented dorsally. Bar, 50  $\mu$ m.

polarized with a broad lagging edge and actin localized at the leading edge (Fig. 1, D and E 5; Fig. S2; and Videos S3 and S4). On average, individual germ cells transmigrated the midgut within 40 min from the onset of polarization. Tracking of individual germ cells showed that they dispersed radially and transmigrated in all directions through the pocket of the midgut epithelium (Fig. 1 F). After transmigration, germ cells reoriented on the midgut toward the dorsal side of the embryo, sorted into two bilateral groups, and migrated toward the gonadal mesoderm, which forms on either side of the embryo, as described previously (Sano et al., 2005).

#### Tre1 GPCR signaling is required for germ cell polarization and dispersal

*Tre1* encodes an orphan GPCR that is required maternally in germ cells for their migration through the midgut epithelium (Kunwar et al., 2003). In embryos from *tre1* mutant females, (hereafter referred to as “mutant embryos”), germ cells failed to cross the midgut epithelium (Fig. 1, G–J). This phenotype could result from a defect in the acquisition of motility by germ cells or in their ability to polarize, disperse, or transmigrate. To dis-

tinguish between these possibilities, we observed *tre1* mutant germ cells live by *in vivo* imaging. At stage 5, *tre1* germ cells showed small protrusions and sporadically crossed the blastoderm with a similar frequency to the wild type (unpublished data; Kunwar et al., 2003). In striking difference to the wild type, however, the *tre1* germ cell cluster did not reorganize at stage 9 and failed to transmigrate to the midgut (compare Fig. 1 K, 1–6, to Fig. 1 E, 1–5; Video 5, available at <http://www.jcb.org/cgi/content/full/jcb.200807049/DC1>). Mutant germ cells did not polarize, and remained in a tight, disorganized group in which germ cells failed to interact with the surrounding midgut cells (see Figs. 3 B and S1).

#### G proteins are downstream mediators of *Tre1* signaling

To begin to understand how *Tre1*, an orphan GPCR, initiates germ cell migration, we asked whether *Tre1* function was mediated by trimeric G protein activation in germ cells (Table S1, available at <http://www.jcb.org/cgi/content/full/jcb.200807049/DC1>). We found that only a single *Gγ* (*Gy1*) and a single *Gβ* (*Gβ13f*) subunit are provided maternally (Table S1; Fuse et al., 2003).

Loss of maternal G $\beta$ 13f or G $\gamma$ 1 function causes defects in gastrulation, which precluded an immediate analysis of germ cell migration (Fig. 2, A and B; Fuse et al., 2003; Yu et al., 2003; Wang et al., 2005). However, we were able to rescue the gastrulation defect through early zygotic, soma-specific expression of the respective G protein (see Materials and methods and Fig. 2 C). This genetic manipulation allowed us to test for a germ cell-specific role of these G proteins, as early *D. melanogaster* germ cells are transcriptionally silent, and germ cells thus depend completely on the maternally provided G proteins. In embryos rescued for the gastrulation defect, G $\beta$ 13f mutant germ cells were unable to disperse and migrate through the midgut epithelium, and thus resembled the *tre1* phenotype (Fig. 2, G–I). G $\gamma$ 1 mutants showed a similar although slightly weaker phenotype likely caused by residual function of the G $\gamma$ 1<sup>N159</sup> allele used, which lacks the C-terminal isoprenylation site required for membrane anchoring (Fig. 2, J–L; Izumi et al., 2004). These results suggest that germ cell transepithelial migration requires Tre1-mediated canonical G protein signaling.

For G $\alpha$  proteins, we focused in particular on the role of the single *D. melanogaster* G $\alpha$ 12/13A homologue, encoded by *concertina* (*cta*), because this subfamily of G proteins has been shown to regulate cell migration and metastatic invasion and to directly interact with E-cadherin and Rho1 (Table S1; Huber et al., 2005; Kelly et al., 2006a,b). Cta protein is present in the germ cells and maternal loss of *cta* causes a gastrulation defect similar to G $\beta$ 13f and G $\gamma$ 1 (Parks and Wieschaus, 1991). Again, we were able to rescue the gastrulation phenotype by early, somatic Cta expression, as described for G $\gamma$ 1 and G $\beta$ 13f (Fig. 2 C). In contrast to our findings with G $\beta$  and G $\gamma$  mutants, however, *cta* mutant germ cells migrated normally to the gonad (Table S1). To confirm this result, we transplanted mutant *cta* germ cells derived from *cta* mutant mothers into wild-type embryos. We found that *cta* germ cells migrated to the gonad with similar efficiency as transplanted wild-type control germ cells (unpublished data). Thus, G $\alpha$ 12/13 does not act as the sole mediator of Tre1 GPCR activation. Our analysis of the available mutants in other G $\alpha$  proteins did not reveal a single G $\alpha$  protein that mediates the Tre1 signal, which perhaps indicates that redundant or overlapping functions of G $\alpha$  proteins act downstream of Tre1 (for details see Table S1).

#### G $\beta$ 13f and G $\gamma$ 1 signaling is required for germ cell polarization, dispersal, and transepithelial migration

Our observation that both G $\beta$ 13f and G $\gamma$ 1 are required for germ cell dispersal and transepithelial migration suggests that Tre1 function in germ cells is mediated by a G protein-dependent pathway, akin to the requirement for GPCR signaling seen during the directed migration of *Dictyostelium discoideum* amoeba and in neutrophils toward a chemokine gradient. To determine how Tre1 signaling may affect downstream components, we analyzed the localization of G $\beta$ 13f protein as well as the localization of Rho1, which we had previously shown to affect germ cell transepithelial migration in wild-type and *tre1* mutant germ cells (Kunwar et al., 2003). We found that G $\beta$ 13f and Rho1 proteins were localized uniformly along the cell membrane of wild-

type germ cells at the blastoderm stage (stage 5; Fig. 3, C, D, K, and L). At stage 9, as wild-type germ cells polarize, G $\beta$ 13f and Rho1 proteins were down-regulated along the germ cell membranes facing the midgut, and became highly enriched in the tail region (Fig. 3, E, F, M, and N). In early germ cells, G $\beta$ 13f and Rho1 proteins were uniformly distributed in *tre1* mutants similar to the wild type (Fig. 3, G, H, O, and P); in contrast to the wild type, however, this uniform distribution persisted during stage 9 (Fig. 3, I, J, Q, and R). These results suggest that Tre1 receptor activation leads to germ cell polarization in part by causing the redistribution of downstream signaling molecules away from the leading edge and accumulation in the tail.

#### Tre1 GPCR signaling controls localization of DE-cadherin

As shown in Fig. 1, *tre1* mutant germ cells failed to disperse at the onset of the migration, which suggests that *tre1* regulates adhesion molecules in germ cells. DE-cadherin is a good candidate, as it is deposited maternally in the early embryo. We first tested the role of DE-cadherin in the adhesion of wild-type germ cells. For this analysis, we used a newly identified partial loss-of-function allele of *D. melanogaster* E-cadherin encoded by the *shotgun* (*shg*) gene, which allows normal oogenesis (see Materials and methods; Tepass et al., 1996; Uemura et al., 1996). In embryos derived from *shg*<sup>A9-49</sup> mutant ovaries, germ cells did not organize into a radial cluster (Fig. 4, G and H). Instead, germ cells separated from one another prematurely, at early stage 8 (3 h and 10 min to 3 h and 40 min AEL) compared with stage 10 in the wild type (4 h and 20 min to 5 h and 20 min AEL; Fig. 4, A–F). This dispersal phenotype was observed in embryos from homozygous germ line clones, in which embryonic patterning defects were rescued by a wild-type *shg*<sup>+</sup> copy from the father (M<sup>–</sup>Z<sup>+</sup>). This suggests that DE-cadherin is required autonomously in germ cells, as they are transcriptionally quiescent and thus likely depend exclusively on maternally contributed DE-cadherin (Van Doren et al., 1998; Martinho et al., 2004). These results indicate that DE-cadherin is required for germ cell–germ cell adhesion in the wild-type embryo.

To understand how DE-cadherin is regulated in the dispersal step, we analyzed the distribution of DE-cadherin in wild-type germ cells. We found that DE-cadherin as well as  $\alpha$  and  $\beta$  catenins were initially uniformly present along the germ cell membrane but became enriched in the tail region during germ cell polarization (Fig. 5, A–C and G–I; and Fig. S3, available at <http://www.jcb.org/cgi/content/full/jcb.200807049/DC1>). In stark contrast, DE-cadherin remained uniformly distributed along the cell surface in *tre1* mutant embryos (Fig. 5, D–F and J–L). To quantitate the levels, we compared the fluorescent intensity of DE-cadherin staining on the cell membrane of wild-type and *tre1* mutant germ cells. We found that DE-cadherin was distributed uniformly and that levels were similar in wild-type and mutant germ cells at stage 5, before migration, whereas the levels were reduced along the leading edge membrane of wild-type germ cells compared with *tre1* mutant germ cells at stage 9 (Fig. 5 M). These results suggest that *tre1* activation leads to a reduction of DE-cadherin along the leading edge and restricts it in the tail region.

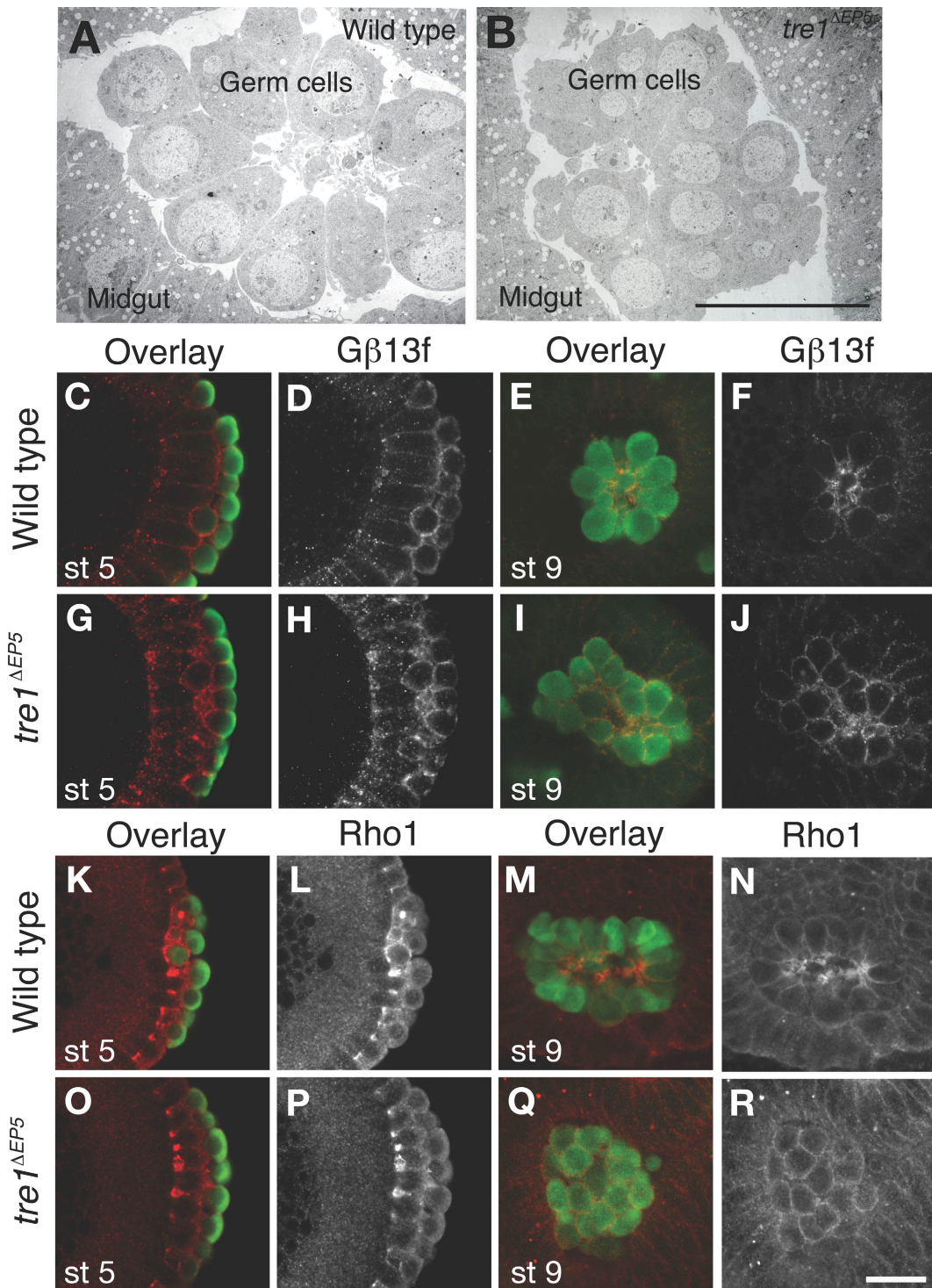


**Figure 3. *Tre1* regulates germ cell polarization and G protein localization.** (A and B) Electron micrograph images of wild-type and *tre1* germ cells at stage 9. Germ cells were identified by the presence of a large nucleus and the lack of white lipid droplets. (A) In wild-type embryos at stage 9, germ cells are organized into a group with little interaction with the surrounding midgut. Germ cells display polarized morphology, with their nuclei facing the midgut and their tails toward the center of the cluster. (B) In *tre1* mutants at stage 9, germ cells are not well organized into a radial cluster and are not polarized like the wild type. (C–J) Gβ13f protein localization in the wild type and *tre1* mutants. At stage 5, Gβ13f protein (red) is uniformly distributed along the cell surface in wild-type (C and D) and *tre1* mutant (G and H) germ cells (green). At stage 9, Gβ13f protein is localized to the tail region of wild-type germ cells (E and F) but is uniformly distributed in *tre1* mutant (I and J) germ cells (Gβ13f channel shown in D, H, F, and J). (K–R) Rho1 protein localization in the wild type and *tre1* mutants. At stage 5, Rho1 protein (red) is uniformly distributed along the cell surface in wild-type (K and L) and *tre1* mutant (O and P) germ cells (green). At stage 9, Rho1 protein is localized to the tail region of wild-type germ cells (M and N) but is uniformly distributed in *tre1* mutant (Q and R) germ cells (Rho1 channel shown in L, P, N, and R). Germ cells are visualized by anti-Vasa antibody (green). Bars, 20  $\mu$ m.

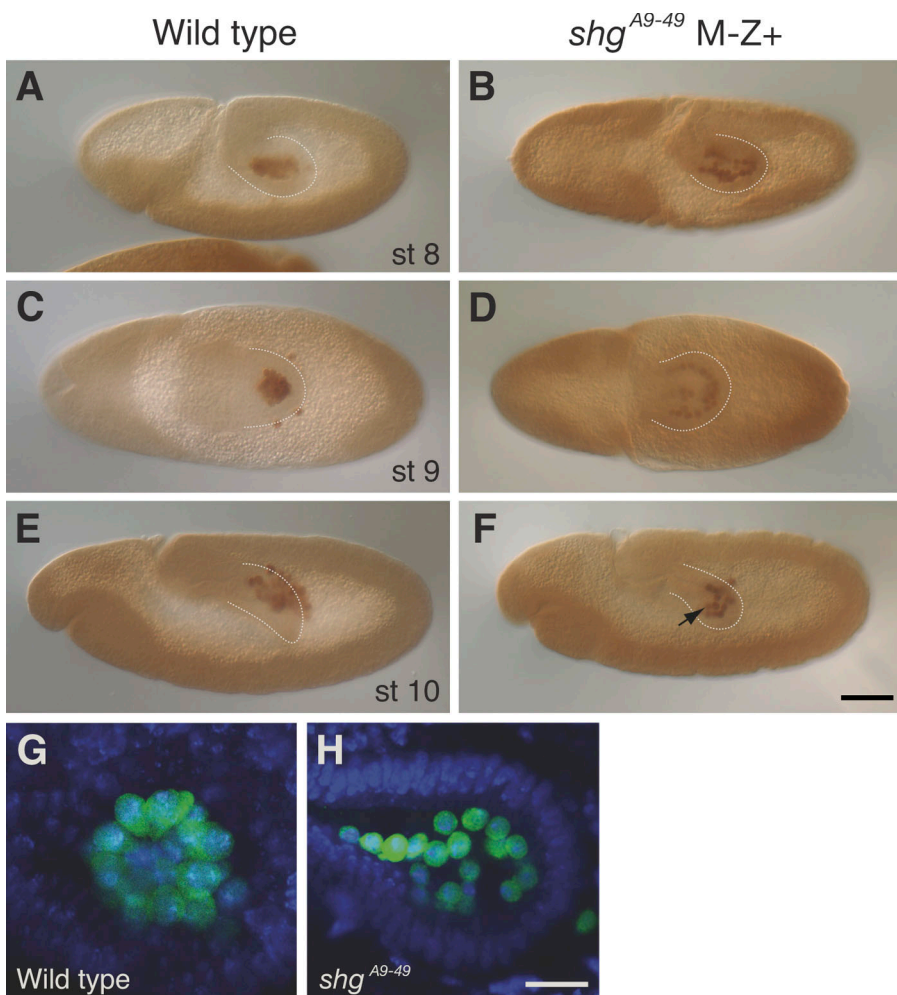


**Figure 4. DE-cadherin is required for germ cell-germ cell adhesion.** (A, C, and E) Wild-type germ cells (brown) form a tight cluster inside the posterior midgut primordium (dotted lines) during stage 8–9 (A and C). Germ cells disperse just before the onset of migration at stage 10 (E). (B, D, and F) In maternal *shg*<sup>A9-49</sup> mutants, germ cells precociously disperse within the midgut, yet they do not initiate premature transmigration (B and D). *shg*<sup>A9-49</sup> mutant germ cells have a slight delay in crossing the midgut, and 38% of embryos displayed partial or no transmigration of germ cells at stage 10 ( $n = 39$ ; arrow in F). (G and H) High-magnification confocal images of germ cells in wild-type (G) and *shg*<sup>A9-49</sup> mutants (H) at stage 9. Note the lack of clear polarization and radial organization in *shg*<sup>A9-49</sup> ( $m^-$ ,  $z^+$ ) mutant germ cells (H). Germ cells were labeled with anti-Vasa antibody (green), and nuclei were labeled with DAPI (blue). Embryos in A, B, E, and F are oriented anterior to the left, lateral view. Embryos in C and D are oriented anterior to the left, dorsal view. Bars, (F) 50  $\mu$ m; (H) 20  $\mu$ m.

#### Reduction in germ cell-germ cell adhesion is necessary but not sufficient for transepithelial migration

In *shg* mutants, early dispersal of germ cells did not lead to premature migration through the midgut, as would be expected if release of germ cell-germ cell adhesion via E-cadherin was the only trigger for transepithelial migration. Instead, *shg* mutant germ cells moved through the midgut slightly later during stage 10 than wild-type germ cells. This delay phenotype is less penetrant (38%,  $n = 39$ ) compared with the precocious dispersal phenotype (93%,  $n = 30$ ) and could be caused by an impaired ability of the *shg*<sup>A9-49</sup> mutant germ cell to migrate at this and subsequent stages (see also Fig. S4, available at <http://www.jcb.org/cgi/content/full/jcb.200807049/DC1>).

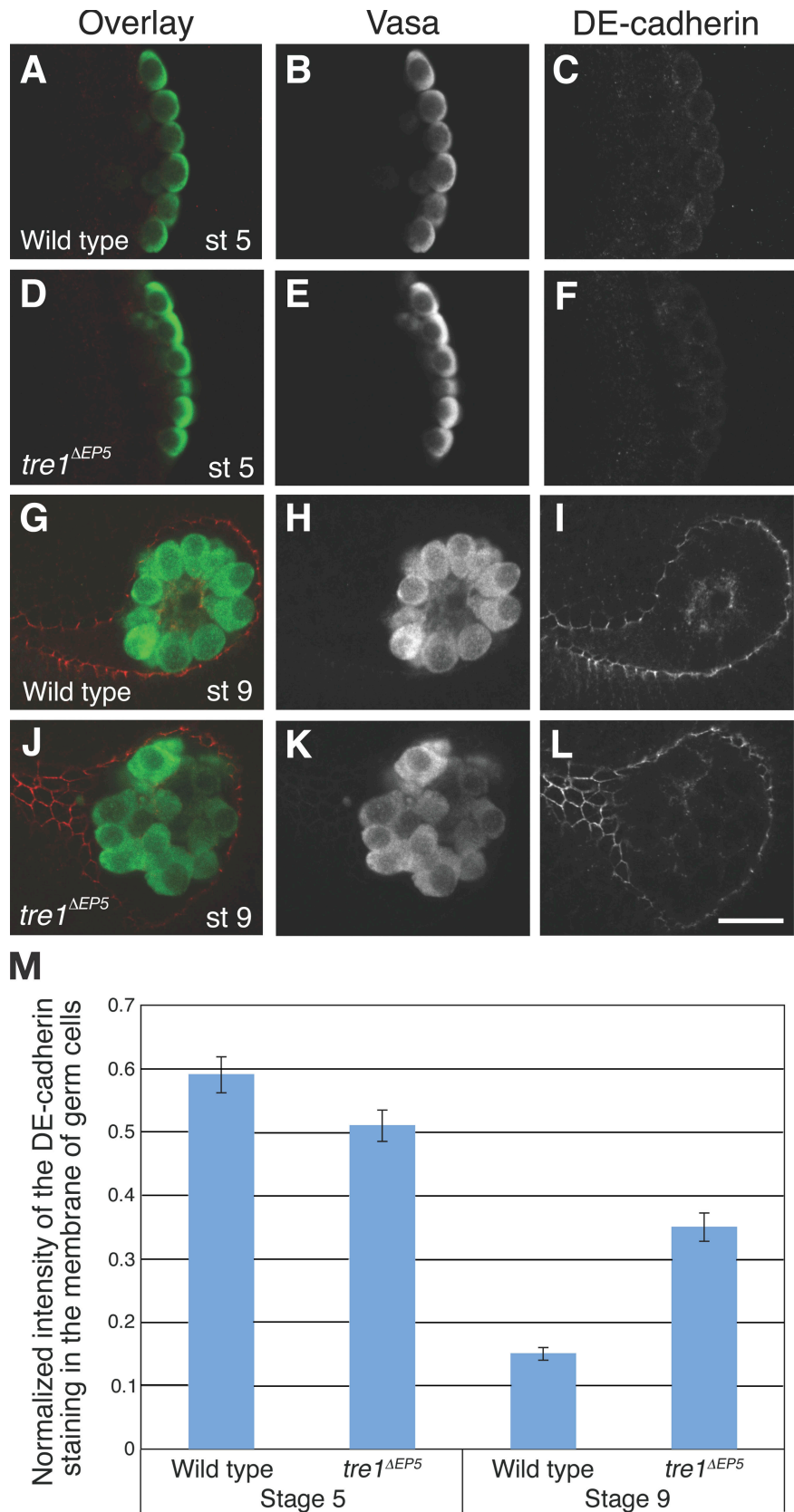
To test directly if Tre1 acts via DE-cadherin in transepithelial migration, we generated embryos that lacked *tre1* and maternal *shg*<sup>A9-49</sup> function. The germ cells in these embryos dispersed early, thus displaying a phenotype similar to *shg*<sup>A9-49</sup> mutants (compare Fig. 6, C and D, to Fig. 4, B, D, and F); 80% of *tre1*, *shg*<sup>A9-49</sup> double mutant embryos showed precocious dispersal as opposed to 0% in the *tre1* mutant embryos ( $n = 42$ ). However, even these dispersed germ cells were not able to transmigrate through the midgut in *tre1*, *shg*<sup>A9-49</sup> double mutant embryos, thereby resembling *tre1* mutant germ cells (Fig. 6, A–D).

This suggests that loss of germ cell-germ cell contact may not be sufficient to trigger transepithelial migration. To test this idea further, we disrupted germ cell-germ cell contact independent of E-cadherin function by reducing the germ cell number. We used alleles of the maternal effect gene *tudor* (*tud*) to reduce the number of germ cells in the embryo to a single germ cell (Arkov et al., 2006). Such single, *tud* mutant germ cells migrated through the midgut and invariably reached the gonad (100%,  $n = 10$ ; Fig. 6, E and F). These germ cells had normal morphology and appeared polarized (Fig. 6, G–I). Next, we analyzed mutant embryos lacking both *tre1* and maternal *tud*. In the absence of *tre1*, single germ cells were left inside the midgut and did not migrate to the gonad (84%,  $n = 38$ ; Fig. 6, J and K). Thus, whereas germ cell individualization requires Tre1-mediated down-regulation of DE-cadherin, Tre1 activity has additional roles in transepithelial migration.

#### Discussion

We have used live imaging to explore the mechanisms by which germ cells acquire motility and traverse the midgut epithelium. We found that before transepithelial migration, germ cells polarize toward the midgut and down-regulate E-cadherin from the leading edge and accumulate E-cadherin in the tail region.

**Figure 5. *tre1* regulates DE-cadherin localization in the tail of germ cells.** (A–F) DE-cadherin localization in wild-type and *tre1* germ cells at stage 5. Embryos were stained with anti-DE-cadherin (red) and anti-Vasa antibodies (green). DE-cadherin is distributed uniformly in the germ cell membrane in the wild type (A–C) and *tre1* mutants (D–F). (G–L) DE-cadherin localization in wild-type and *tre1* germ cells at stage 9. In wild-type germ cells, DE-cadherin is enriched in the tail region (G–I). In *tre1* mutant germ cells, DE-cadherin is evenly distributed in the cell membrane (J–L). Vasa channel is shown in B, E, H, and K, and the DE-cadherin channel is shown in C, F, I, and L. (M) Quantification of DE-cadherin levels in the cell body membrane of stage 5 and 9 germ cells. Normalized intensity of the DE-cadherin staining is shown (see Materials and methods). DE-cadherin levels are similar in wild-type and *tre1* germ cells at stage 5. At stage 9, DE-cadherin levels in *tre1* mutant germ cells are significantly higher than wild-type cells. Error bars indicate standard error. Bar, 20  $\mu$ m.



This polarization requires Tre1 GPCR activity. We propose that GPCR-mediated polarization triggers germ cell dispersal and orients germ cells toward the midgut for directed transepithelial migration.

A requirement for GPCR signaling during the directed migration toward a chemokine gradient has been described in detail in *D. discoideum* amoeba and in mammalian neutrophils.

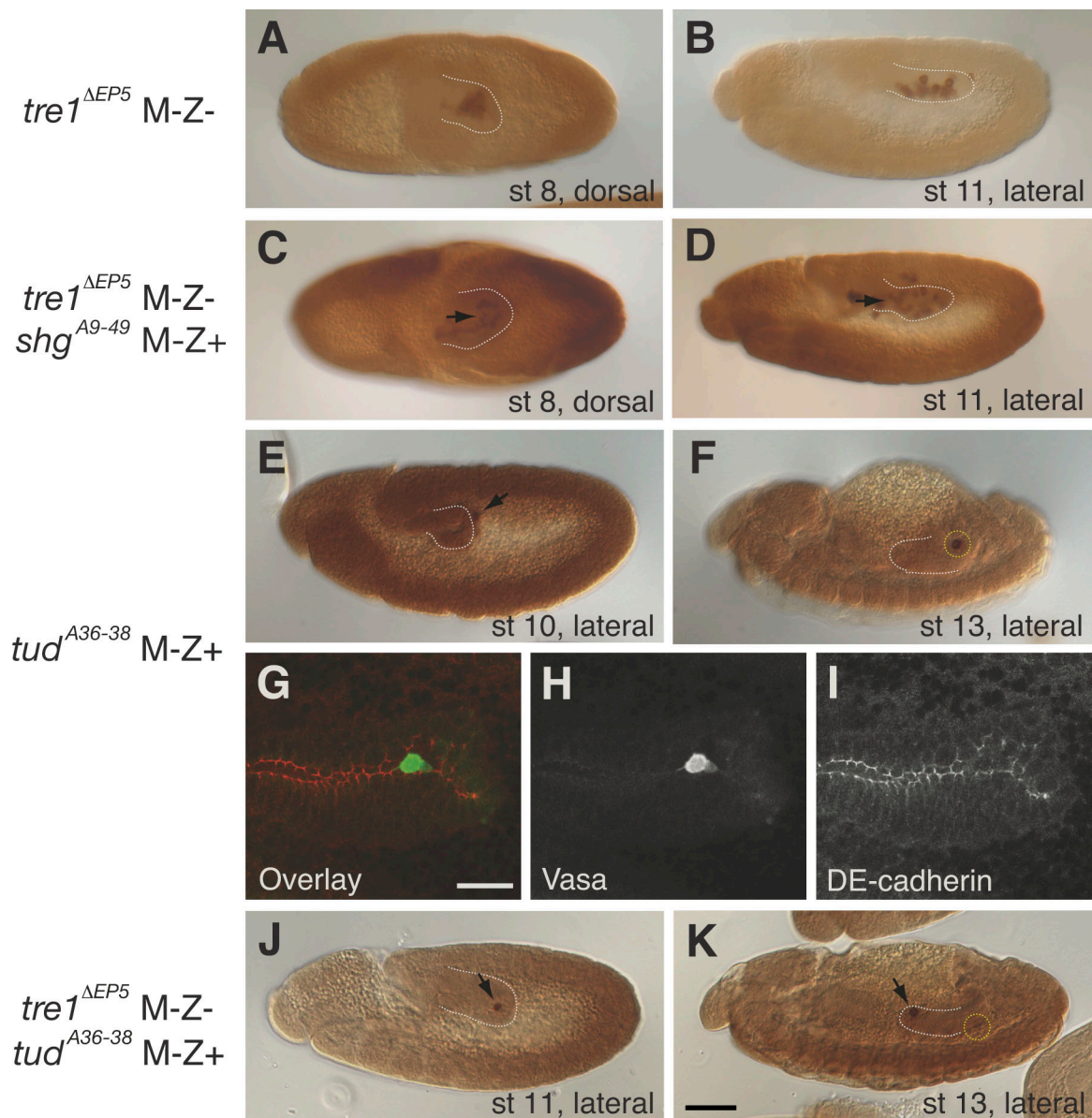


**Figure 6. Reduction of DE-cadherin function or adhesion between germ cells does not rescue the *tre1* phenotype.** (A and B) In *tre1* mutants, germ cells (brown) form a tight cluster inside the midgut (white dotted lines in A–F, J, and K) during stages 8–11. (C and D) In *tre1* and maternal *shg*<sup>A9-49</sup> double mutants, germ cells disperse within the midgut (C, arrow); however, they are not able to migrate through the midgut (D, arrow). (E and F) Single germ cells in maternal *tud*<sup>A36-38</sup> mutants cross the midgut normally (E, arrow) to reach the gonad (F, yellow dotted circle). (G–I) Polarity of single germ cells. Maternal *tud*<sup>A36-38</sup> mutant embryos were stained with anti-Vasa (green) and anti-DE-cadherin antibodies (red). Single germ cells display a polarized morphology with a tail at stage 9. Vasa channel is shown in H, and the DE-cadherin channel is shown in I. (J and K) Single germ cells (arrows) in *tre1* and maternal *tud*<sup>A36-38</sup> double mutants fail to migrate through the midgut. Embryos are oriented anterior to the left, lateral view in all panels, except for embryos in A and C, which are oriented dorsally. Bars: (G) 20  $\mu$ m; (K) 50  $\mu$ m.

The events underlying signal transduction leading to the polarization of migrating cells have been worked out extensively in these cells. The first localized response to receptor activation is the enrichment of the activated G protein  $\beta\gamma$  subunits, which results in the activation of phosphoinositide 3 (PI3) kinase. As a consequence of chemokine sensing, the PI3 kinase product phosphatidylinositol 3,4,5-tris phosphate (PIP3) becomes localized to the leading edge, and the phosphatase PTEN (phosphatase and tensin homolog) moves to the lagging edge in a Rho dependent manner (for review see Affolter and Weijer, 2005). These signaling events organize the cytoskeleton leading to cellular polarization and di-

rectional movement. Our studies suggest a new mechanism by which GPCR signaling initiates directed cell migration. We find that activation of Tre1 causes a redistribution of G protein  $\beta$ , the GTPase Rho1, DE-cadherin, and other adherens junction components to a small region in the tail of the germ cells. The decrease in DE-cadherin from the leading edge of germ cells causes a loss of adhesion across the broad leading edge of the germ cells and causes germ cell polarization toward the midgut. This localization event may thereby convert an adherent group of cells into directionally migrating individuals. Tre1 belongs to a family of GPCRs that includes Moody in *D. melanogaster* and GPR84 in

mouse and human (Bainton et al., 2005; Bouchard et al., 2007). Based on our results with Tre1, this family may act to regulate cellular polarity and adhesion, a view in line with the proposed function of Moody in epithelial morphology at the blood–brain barrier, and with GPR84, which was recently described to be up-regulated in microglia upon infection (Schwabe et al., 2005; Bouchard et al., 2007).

How could Tre1 activation cause DE-cadherin redistribution? Regulation of E-cadherin is widely attributed to play an important role in metastasis and in the epithelial-to-mesenchymal transition that occurs during gastrulation and neural crest migration. In these systems, it has been proposed that E-cadherin is regulated by transcriptional repression or by Gα12/13-mediated uptake and turnover (Huber et al., 2005; Kelly et al., 2006a,b). Our data suggest the presence of a different mode of regulation, as neither transcriptional regulation nor Gα12/13 activity seem to be required for the regulation of DE-cadherin in germ cells. An attractive mechanism for DE-cadherin down-regulation could be the control of its endocytosis by Tre1. During zebrafish gastrulation, Rab GTPases have been shown to control E-cadherin turnover and the adhesion of mesendodermal cells (Ulrich et al., 2005). A role for Rab proteins in germ cell migration has yet to be demonstrated. We find the same localization pattern for Gβ13f, Rho1, and DE-cadherin in the wild type, and this pattern is disrupted in *tre1* mutant germ cells. This suggests a role for G protein and Rho1 activation in the polarization of DE-cadherin in germ cells.

Tre1 also affects transepithelial migration independently of global DE-cadherin regulation. We show that uniform down-regulation of DE-cadherin or loss of germ cell–germ cell contact in single cells are neither sufficient to trigger precocious transepithelial migration in the wild type nor able to suppress the *tre1* transepithelial migration phenotype. One possibility is that the localized activation of Tre1 and polarized down-regulation of DE-cadherin at the leading edge would orient germ cells radially toward the midgut. This radial orientation would allow germ cells to respond to additional guidance cues required for directed transepithelial migration. Although these additional guidance cues may not depend on DE-cadherin, they require G protein signaling and Tre1.

A function for E-cadherin in controlling adhesion and migration has been studied extensively in the progression of tumor metastasis and the development of epithelial–mesenchymal transitions (EMTs; Radisky, 2005; Thiery and Sleeman, 2006). Cells undergoing metastasis and EMTs express lower levels of E-cadherin, and the loss of E-cadherin promotes invasion of tumor cells (Yang et al., 2004; Zhang et al., 2006). The loss of E-cadherin in these cases promotes the disruption of E-cadherin-mediated cell adhesion between epithelial cells, allowing these cells to spread and migrate, and is often triggered through induction of the transcriptional repressors Twist and Snail in response to inductive signals (Yang et al., 2004). However, in the case of germ cell dispersal, the effect of Tre1 on DE-cadherin is not transcriptional because DE-cadherin is provided maternally in the germ cells. Our data suggest that Tre1 GPCR signaling might regulate the turnover or cellular distribution of DE-cadherin-mediated adhesion complexes in a polarized fashion. It is pos-

sible that in addition to transcriptional mechanisms, such a polarized regulation also functions during EMT and metastasis.

## Materials and methods

### Fly stocks and genetics

*P<sub>nos</sub>::egfp-moe::nos* 3' untranslated region was used to label germ cells with EGFP for live imaging (Sano et al., 2005). *tre1<sup>ΔEP5</sup>* is a deletion lacking the first exons of the *tre1* and the *Gr5a* genes (Ueno et al., 2001; Kunwar et al., 2003). The polarity defect in *tre1* germ cells was rescued by a genomic fragment including the *tre1* gene but not the *Gr5a* gene. *tud<sup>A36-38</sup>* was identified in a maternal-effect screen on the 2R chromosome (Barbosa et al., 2007). *tud<sup>A36-38</sup>* females produce embryos with reduced numbers of germ cells. *Gβ13f<sup>Δ15</sup>* was generated by imprecise excision of *l(1)G0369* and is a null allele deleting the open reading frame of the *Gβ13f* gene (provided by N. Fuse, Kyoto University, Kyoto, Japan; Fuse et al., 2003). *Gy1<sup>N159</sup>* is a nonsense mutation in the *Gy1* gene (provided by F. Matsuzaki, Center for Developmental Biology, Riken, Kobe, Japan; Izumi et al., 2004). Upstream activation sequence (UAS)-*Gβ13f* and UAS-*Gy1* were used to rescue the gastrulation defects in maternal *Gβ13f* and *Gy1* mutants (Fuse et al., 2003). UAS-*cta* used to rescue the gastrulation defects in maternal *concertina* mutants was provided by N. Fuse. *nullo-GAL4* flies were obtained from E. Wieschaus (Princeton University, Princeton, NJ) and W. Gehring (Biozentrum, Basel, Switzerland; Kunwar et al., 2003). *shg<sup>A949</sup>* was isolated in a 2R maternal-effect screen (Barbosa et al., 2007). *shg<sup>A949</sup>* was identified as an allele of *shg* based on noncomplementation for lethality of *shg<sup>P341</sup>* and *shg<sup>H</sup>*, and the deficiencies *Exel16071* and *Exel16072*, which uncover only *shg* (Tepass et al., 1996; Uemura et al., 1996). Sequencing of the genomic DNA identified a missense mutation in the second extracellular cadherin domain (K336E) in the *shg<sup>A949</sup>* allele. *shg<sup>A949</sup>* germ line clones were induced by the flipase recombination target (FLP) OvoD method (Chou and Perrimon, 1996). To generate *shg<sup>A949</sup>* germ line clones in a *tre1* mutant background, *hs-flp22* on the X chromosome was recombined with *tre1<sup>ΔEP5</sup>*.

### Live imaging

Live imaging was performed as described previously (Sano et al., 2005). Embryos were collected at room temperature (22°C) and dechorionated with 50% bleach for 5 min. The dechorionated embryos were mounted in Halocarbon 200 oil (Halocarbon) on an oxygen permeable membrane (YSL Inc.) and covered with a 1.5-μM coverslip. Images were acquired in multiphoton system (Radiance; BioRad Laboratories) with a microscope (Eclipse E600FN; Nikon) and a 10-W pumped Tsunami laser (Newport Corp.) controlled by Laser Sharp software (BioRad Laboratories). Objectives used were 40× (Plan Fluor, water, 0.75 NA; Nikon) and 60× (Plan Apo, water, 1.2 NA; Nikon). The time-lapse images were processed to make videos using the Velocity 2.6.1 software (Improvision). Migratory paths of germ cells were traced manually using Photoshop software (Adobe).

### Electron microscopy

A detailed procedure for electron microscopy has been described previously (Arkov et al., 2006). 1-h egg layings were aged for 4–5 h at room temperature before fixation. The stage and orientation of the embryo were determined in 2-μm semithin sections. Ultrathin (80-nm) sections were cut on an ultramicrotome (Ultracut UCT; Reichert), stained with uranyl acetate followed by lead citrate, and viewed on a transmission electron microscope (1200EX; JEOL Ltd.) at 80 kV.

### Immunohistochemistry

Antibody staining of embryos was performed as described previously (Stein et al., 2002), except for anti-DE-cadherin staining, in which we fixed embryos with calcium and devitellinized embryos with ethanol (Oda et al., 1993). The following antibodies were used (dilutions follow in parenthesis): rabbit anti-Vasa (1:10,000; provided by A. Williamson and H. Zinszner, New York University School of Medicine, New York, NY), rat anti-DE-cadherin (DCAD2; 1:50; Developmental Studies Hybridoma Bank), rabbit anti-Gβ13f (1:500; provided by N. Fuse; Fuse et al., 2003), Rho1 antibody, and mouse anti-neurotactin (BP106; 1:200; Developmental Studies Hybridoma Bank). For staining with anti-neurotactin, embryos were heat-fixed as described previously (Eldon and Pirrotta, 1991; Stein et al., 2002). Secondary antibodies used were: biotinylated goat anti-rabbit antibody (1:500; Jackson ImmunoResearch Laboratories), Alexa Fluor 488-conjugated goat anti-rabbit antibody (1:500; Invitrogen), Cy3-conjugated donkey anti-rat

antibody (1:500; Jackson ImmunoResearch Laboratories), and Cy3-conjugated donkey anti-mouse antibody (1:500; Jackson ImmunoResearch Laboratories). DAPI staining was done after the secondary antibody reaction (1:1,000; Roche). Antibody detection for the biotinylated antibody was performed with the Vectastain Elite ABC Standard kit (Vector Laboratories). Embryos were observed with an Axiophoto microscope (Carl Zeiss, Inc.) and were photographed with a charge-coupled device camera (14.2 Color Mosaic; Insight 4; Diagnostics Instruments, Inc.) using Spot version 4.5 software (Diagnostics Instruments, Inc.). Fluorescent signal was observed with a confocal microscope (LSM510; Carl Zeiss, Inc.).

### Quantification of the DE-cadherin staining

Wild-type and *tre1* mutant embryos were stained with anti-DE-cadherin and anti-Vasa antibodies. Embryos were scanned with an LSM510 confocal microscope, and the intensity of the DE-cadherin staining in the germ cell membrane was measured with LSM510 software. The intensity of DE-cadherin staining in the germ cell membrane was normalized by an internal standard, namely the intensity of DE-cadherin at the apical membrane of polarized somatic cells (blastoderm cells for stage 5 or posterior midgut cells for stage 9), which seemed unaffected in *tre1*. An arbitrary intensity scale, set as 1 for the intensity of the internal standard, was used in Fig. 5. Four germ cells and two midgut areas were analyzed per embryo, and 14 wild-type and 15 *tre1* mutant embryos were analyzed each for stages 5 and 9 in Fig. 5 M.

### Online supplemental material

Fig. S1 shows electron micrographs demonstrating germ cell dispersal, interaction between germ cells and posterior midgut in the wild-type embryo, and tight association between germ cells, as well as the failure of germ cells to interact with midgut in *tre1* mutant. Fig. S2 shows still images of a video showing dispersal and amoeboid migration of wild-type germ cells at the onset of transepithelial migration. Fig. S3 shows that, like E-cadherin,  $\beta$ -catenin and  $\alpha$ -catenin also accumulate in the tail of wild-type germ cells at stage 9. Fig. S4 shows additional phenotypes of *shg*<sup>A949</sup> during later stages of embryogenesis, when germ cells separate into two bilateral clusters and associate with the somatic gonad. Table S1 summarizes the expression patterns of the *D. melanogaster*  $G\alpha$ ,  $G\beta$ , and  $G\gamma$  proteins and describes the respective loss-of-function phenotypes in general and in germ cells. Video 1 shows behavior of wild-type germ cells during the blastoderm stage. Video 2 shows behavior of wild-type germ cells during the gastrulation stage. Video 3 shows polarization and transepithelial migration of germ cells in a wild-type embryo. Video 4 shows the transepithelial migration of germ cells with long extensions in a wild-type embryo. Video 5 shows transepithelial migration of germ cells in an embryo from a *tre1* mutant female. Online supplemental material is available at <http://www.jcb.org/cgi/content/full/jcb.200807049/DC1>.

We are particularly grateful to Dr. Daria Siekhaus for helpful discussion throughout this work and editing of the manuscript. We would like to thank the Bloomington Stock Center for fly stocks, and the Berkeley Drosophila Genome Project for sequence and *in situ* expression data. We also thank Drs. Mike Dustin and Wenbiao Gan, and their laboratory members for help with two-photon microscopy; and Dr. Frank Macaluso, Leslie Gunther, and Juan Jimenez of the Albert Einstein College of Medicine Analytical Imaging Center for assistance with electron microscopy. We are grateful to all members of the Lehmann laboratory, particularly the member of the 2R screen (Alexey Arkov, Elena Arkova, Helene Zinszner, and Thomas Marty) for isolating the *shg*<sup>A949</sup> allele. We are also grateful to Drs. Holger Knaut and Thomas Marty for discussions.

This work was supported by National Institutes of Health grant HD49100. A.D. Renault was a Charles H. Revson Senior Fellow in Biomedical Science. V. Barbosa was supported by the Fundação para a Ciência e Tecnologia, Portugal, and R. Lehmann is a Howard Hughes Medical Institute investigator and a member of the Kimmel Center for Stem Cell Biology.

Submitted: 9 July 2008

Accepted: 4 September 2008

## References

Affolter, M., and C.J. Weijer. 2005. Signaling to cytoskeletal dynamics during chemotaxis. *Dev. Cell.* 9:19–34.

Ara, T., Y. Nakamura, T. Egawa, T. Sugiyama, K. Abe, T. Kishimoto, Y. Matsui, and T. Nagasawa. 2003. Impaired colonization of the gonads by primordial germ cells in mice lacking a chemokine, stromal cell-derived factor-1 (SDF-1). *Proc. Natl. Acad. Sci. USA.* 100:5319–5323.

Arkov, A.L., J.Y. Wang, A. Ramos, and R. Lehmann. 2006. The role of Tudor domains in germline development and polar granule architecture. *Development.* 133:4053–4062.

Bainton, R.J., L.T. Tsai, T. Schwabe, M. DeSalvo, U. Gaul, and U. Heberlein. 2005. *moody* encodes two GPCRs that regulate cocaine behaviors and blood-brain barrier permeability in *Drosophila*. *Cell.* 123:145–156.

Barbosa, V., N. Kimm, and R. Lehmann. 2007. A maternal screen for genes regulating *Drosophila* oocyte polarity uncovers new steps in meiotic progression. *Genetics.* 176:1967–1977.

Boldajipour, B., H. Mahabaleshwar, E. Kardash, M. Reichman-Fried, H. Blaser, S. Minina, D. Wilson, Q. Xu, and E. Raz. 2008. Control of chemokine-guided cell migration by ligand sequestration. *Cell.* 132:463–473.

Bouchard, C., J. Page, A. Bedard, P. Tremblay, and L. Vallières. 2007. G protein-coupled receptor 84, a microglia-associated protein expressed in neuroinflammatory conditions. *Glia.* 55:790–800.

Chou, T.B., and N. Perrimon. 1996. The autosomal FLP-DFS technique for generating germline mosaics in *Drosophila melanogaster*. *Genetics.* 144:1673–1679.

Chung, C.Y., S. Funamoto, and R.A. Firtel. 2001. Signaling pathways controlling cell polarity and chemotaxis. *Trends Biochem. Sci.* 26:557–566.

Doitsidou, M., M. Reichman-Fried, J. Stebler, M. Koprucker, J. Dorries, D. Meyer, C.V. Esguerra, T. Leung, and E. Raz. 2002. Guidance of primordial germ cell migration by the chemokine SDF-1. *Cell.* 111:647–659.

Eldon, E.D., and V. Pirrotta. 1991. Interactions of the *Drosophila* gap gene giant with maternal and zygotic pattern-forming genes. *Development.* 111:367–378.

Franz, C.M., G.E. Jones, and A.J. Ridley. 2002. Cell migration in development and disease. *Dev. Cell.* 2:153–158.

Friedl, P., and K. Wolf. 2003. Tumour-cell invasion and migration: diversity and escape mechanisms. *Nat. Rev. Cancer.* 3:362–374.

Fuse, N., K. Hisata, A.L. Katzen, and F. Matsuzaki. 2003. Heterotrimeric G proteins regulate daughter cell size asymmetry in *Drosophila* neuroblast divisions. *Curr. Biol.* 13:947–954.

Horwitz, R., and D. Webb. 2003. Cell migration. *Curr. Biol.* 13:R756–R759.

Huber, M.A., N. Kraut, and H. Beug. 2005. Molecular requirements for epithelial-mesenchymal transition during tumor progression. *Curr. Opin. Cell Biol.* 17:548–558.

Iijima, M., Y.E. Huang, and P. Devreotes. 2002. Temporal and spatial regulation of chemotaxis. *Dev. Cell.* 3:469–478.

Izumi, Y., N. Ohta, A. Itoh-Furuya, N. Fuse, and F. Matsuzaki. 2004. Differential functions of G protein and Baz-aPKC signaling pathways in *Drosophila* neuroblast asymmetric division. *J. Cell Biol.* 164:729–738.

Kelly, P., B.J. Moeller, J. Juneja, M.A. Booden, C.J. Der, Y. Daaka, M.W. Dewhirst, T.A. Fields, and P.J. Casey. 2006a. The G12 family of heterotrimeric G proteins promotes breast cancer invasion and metastasis. *Proc. Natl. Acad. Sci. USA.* 103:8173–8178.

Kelly, P., L.N. Stemmle, J.F. Madden, T.A. Fields, Y. Daaka, and P.J. Casey. 2006b. A role for the G12 family of heterotrimeric G proteins in prostate cancer invasion. *J. Biol. Chem.* 281:26483–26490.

Knaut, H., C. Werz, R. Geisler, and C. Nusslein-Volhard. 2003. A zebrafish homologue of the chemokine receptor Cxcr4 is a germ-cell guidance receptor. *Nature.* 421:279–282.

Kunwar, P.S., and R. Lehmann. 2003. Developmental biology: Germ-cell attraction. *Nature.* 421:226–227.

Kunwar, P.S., M. Starz-Gaiano, R.J. Bainton, U. Heberlein, and R. Lehmann. 2003. *Tre1*, a G protein-coupled receptor, directs transepithelial migration of *Drosophila* germ cells. *PLoS Biol.* 1:E80.

Kunwar, P.S., D.E. Siekhaus, and R. Lehmann. 2006. In vivo migration: a germ cell perspective. *Annu. Rev. Cell Dev. Biol.* 22:237–265.

Martinho, R.G., P.S. Kunwar, J. Casanova, and R. Lehmann. 2004. A noncoding RNA is required for the repression of RNApolII-dependent transcription in primordial germ cells. *Curr. Biol.* 14:159–165.

Molyneaux, K.A., H. Zinszner, P.S. Kunwar, K. Schaible, J. Stebler, M.J. Sunshine, W. O'Brien, E. Raz, D. Littman, C. Wylie, and R. Lehmann. 2003. The chemokine SDF1/CXCL12 and its receptor CXCR4 regulate mouse germ cell migration and survival. *Development.* 130:4279–4286.

Montell, D.J. 2006. The social lives of migrating cells in *Drosophila*. *Curr. Opin. Genet. Dev.* 16:374–383.

Moser, B., M. Wolf, A. Walz, and P. Loetscher. 2004. Chemokines: multiple levels of leukocyte migration control. *Trends Immunol.* 25:75–84.

Oda, H., T. Uemura, K. Shiomi, A. Nagafuchi, S. Tsukita, and M. Takeichi. 1993. Identification of a *Drosophila* homologue of  $\alpha$ -catenin and its association with the armadillo protein. *J. Cell Biol.* 121:1133–1140.

Parks, S., and E. Wieschaus. 1991. The *Drosophila* gastrulation gene *concertina* encodes a G alpha-like protein. *Cell.* 64:447–458.

Radisky, D.C. 2005. Epithelial-mesenchymal transition. *J. Cell Sci.* 118:4325–4326.

Raz, E., and M. Reichman-Fried. 2006. Attraction rules: germ cell migration in zebrafish. *Curr. Opin. Genet. Dev.* 16:355–359.

Ridley, A.J., M.A. Schwartz, K. Burridge, R.A. Firtel, M.H. Ginsberg, G. Borisy, J.T. Parsons, and A.R. Horwitz. 2003. Cell migration: integrating signals from front to back. *Science.* 302:1704–1709.

Rorth, P. 2002. Initiating and guiding migration: lessons from border cells. *Trends Cell Biol.* 12:325–331.

Sahai, E. 2005. Mechanisms of cancer cell invasion. *Curr. Opin. Genet. Dev.* 15:87–96.

Sano, H., A.D. Renault, and R. Lehmann. 2005. Control of lateral migration and germ cell elimination by the *Drosophila melanogaster* lipid phosphate phosphatases Wunen and Wunen 2. *J. Cell Biol.* 171:675–683.

Santos, A.C., and R. Lehmann. 2004. Germ cell specification and migration in *Drosophila* and beyond. *Curr. Biol.* 14:R578–R589.

Schwab, S.R., J.P. Pereira, M. Matloubian, Y. Xu, Y. Huang, and J.G. Cyster. 2005. Lymphocyte sequestration through S1P lyase inhibition and disruption of S1P gradients. *Science.* 309:1735–1739.

Schwabe, T., R.J. Bainton, R.D. Fetter, U. Heberlein, and U. Gaul. 2005. GPCR signaling is required for blood-brain barrier formation in *Drosophila*. *Cell.* 123:133–144.

Stein, J.A., H.T. Brothier, L.A. Moore, and R. Lehmann. 2002. Slow as molasses is required for polarized membrane growth and germ cell migration in *Drosophila*. *Development.* 129:3925–3934.

Tepass, U., E. Gruszynski-DeFeo, T.A. Haag, L. Omatyar, T. Torok, and V. Hartenstein. 1996. shotgun encodes *Drosophila* E-cadherin and is preferentially required during cell rearrangement in the neurectoderm and other morphogenetically active epithelia. *Genes Dev.* 10:672–685.

Thiery, J.P., and J.P. Sleeman. 2006. Complex networks orchestrate epithelial-mesenchymal transitions. *Nat. Rev. Mol. Cell Biol.* 7:131–142.

Uemura, T., H. Oda, R. Kraut, S. Hayashi, Y. Kotoaka, and M. Takeichi. 1996. Zygotic *Drosophila* E-cadherin expression is required for processes of dynamic epithelial cell rearrangement in the *Drosophila* embryo. *Genes Dev.* 10:659–671.

Ueno, K., M. Ohta, H. Morita, Y. Mikuni, S. Nakajima, K. Yamamoto, and K. Isono. 2001. Trehalose sensitivity in *Drosophila* correlates with mutations in and expression of the gustatory receptor gene Gr5a. *Curr. Biol.* 11:1451–1455.

Ulrich, F., M. Krieg, E.M. Schotz, V. Link, I. Castanon, V. Schnabel, A. Taubenberger, D. Mueller, P.H. Puech, and C.P. Heisenberg. 2005. Wnt11 functions in gastrulation by controlling cell cohesion through Rab5c and E-cadherin. *Dev. Cell.* 9:555–564.

Van Doren, M., A.L. Williamson, and R. Lehmann. 1998. Regulation of zygotic gene expression in *Drosophila* primordial germ cells. *Curr. Biol.* 8:243–246.

Van Haastert, P.J., and P.N. Devreotes. 2004. Chemotaxis: signalling the way forward. *Nat. Rev. Mol. Cell Biol.* 5:626–634.

Wang, H., K.H. Ng, H. Qian, D.P. Siderovski, W. Chia, and F. Yu. 2005. Ric-8 controls *Drosophila* neural progenitor asymmetric division by regulating heterotrimeric G proteins. *Nat. Cell Biol.* 7:1091–1098.

Wei, S.H., H. Rosen, M.P. Matheu, M.G. Sanna, S.K. Wang, E. Jo, C.H. Wong, I. Parker, and M.D. Cahalan. 2005. Sphingosine 1-phosphate type 1 receptor agonism inhibits transendothelial migration of medullary T cells to lymphatic sinuses. *Nat. Immunol.* 6:1228–1235.

Yang, J., S.A. Mani, J.L. Donaher, S. Ramaswamy, R.A. Itzykson, C. Come, P. Savagner, I. Gitelman, A. Richardson, and R.A. Weinberg. 2004. Twist, a master regulator of morphogenesis, plays an essential role in tumor metastasis. *Cell.* 117:927–939.

Yu, F., Y. Cai, R. Kaushik, X. Yang, and W. Chia. 2003. Distinct roles of G $\alpha$ i and G $\beta$ 13F subunits of the heterotrimeric G protein complex in the mediation of *Drosophila* neuroblast asymmetric divisions. *J. Cell Biol.* 162:623–633.

Zhang, W., A. Alt-Holland, A. Margulis, Y. Shamis, N.E. Fusenig, U. Rodeck, and J.A. Garlick. 2006. E-cadherin loss promotes the initiation of squamous cell carcinoma invasion through modulation of integrin-mediated adhesion. *J. Cell Sci.* 119:283–291.

Zou, Y.R., A.H. Kottmann, M. Kuroda, I. Taniuchi, and D.R. Littman. 1998. Function of the chemokine receptor CXCR4 in hematopoiesis and in cerebellar development. *Nature.* 393:595–599.